

# Synthesis of $\text{Sr}_4\text{Al}_2\text{O}_7:\text{Eu}^{2+}/\text{Dy}^{3+}$ phosphors by the solid-state reaction and luminescent properties

Zhijian Liu<sup>1</sup> · Sijia Chen<sup>2</sup> · Lingbin Meng<sup>1</sup> · Boxiang Liu<sup>1</sup>

Received: 9 April 2015 / Accepted: 19 May 2015 / Published online: 24 May 2015  
© Springer Science+Business Media New York 2015

**Abstract**  $\text{Sr}_4\text{Al}_2\text{O}_7:\text{Eu}^{2+}/\text{Dy}^{3+}$  phosphors are synthesized by the solid-state reaction. The obtained powders are characterized by XRD, SEM and luminescent spectrometer. The effects of the mole ratios of  $\text{Dy}^{3+}/\text{Eu}^{2+}$  on luminescent properties of  $\text{Sr}_4\text{Al}_2\text{O}_7:\text{Eu}^{2+}/\text{Dy}^{3+}$  phosphors are investigated. The XRD pattern indicates that the powders have pure  $\text{Sr}_4\text{Al}_2\text{O}_7$  phase. The SEM micrographs reveal that  $\text{Sr}_4\text{Al}_2\text{O}_7:\text{Eu}^{2+}/\text{Dy}^{3+}$  phosphors show similar irregular morphology. Under the excitation of 360 nm,  $\text{Sr}_4\text{Al}_2\text{O}_7:\text{Eu}^{2+}/\text{Dy}^{3+}$  phosphors exhibit the characteristic emission band originating from the  $4f^65d^1 \rightarrow 4f^7$  transition of  $\text{Eu}^{2+}$  ions. The emission intensity increases with the increasing mole ratio of  $\text{Dy}^{3+}/\text{Eu}^{2+}$  up to 3 and then decreases. Thermoluminescence results indicate that the persistent afterglow of  $\text{Sr}_4\text{Al}_2\text{O}_7:\text{Eu}^{2+}/\text{Dy}^{3+}$  phosphors is generated by suitable electron traps formed by the  $\text{Dy}^{3+}$  ions within the host.

## 1 Introduction

Double oxides containing strontium and aluminium (strontium aluminates) are of interest in materials science because of their uses as long duration photoluminescence or thermoluminescence pigments [1]. In the past few years,

phosphors activated with rare earth metals also have been investigated widely on account of their technological importance [2]. And strontium aluminates have been proved to be of good hosts for rare earth metals and rare earth metals doped strontium aluminates have been synthesized by different methods [2–11]. It is known that the Al/Sr ratio in the strontium aluminates phosphors can affect the long duration phosphorescence. The emission spectra of the samples shift to yellow-green long wavelength from bluish-green-ultraviolet short wave with the increase of Al/Sr ratios resulting from the change in the composition [11]. That is to say, there will be different luminescent properties when the same type of rare earth metal doped into strontium aluminates with different Al/Sr ratios.

$\text{Eu}^{2+}$  ion has a  $4f^7$  electron configuration, and its emission has close relation with the crystal field strength [12]. Generally, the energy of the excited state  $4f^65d^1$  of the  $\text{Eu}^{2+}$  ion is lower than that of the lowest excited state  $^6P$  in the  $4f^7$  electron configuration. As a result, the  $\text{Eu}^{2+}$  ions in most of the compounds present broad band emissions originating from the  $4f^65d^1 \rightarrow 4f^7$  transitions. Moreover, the 5d states of  $\text{Eu}^{2+}$  ions are outer orbitals and the coordination surroundings in the host have a prominent influence on its energies, which induces the emission color from the  $4f^65d^1 \rightarrow 4f^7$  transition of  $\text{Eu}^{2+}$  ion can also vary from ultraviolet to yellow/red light. Moreover, the addition of a certain amount of co-activators can enhance the initial intensity of luminescence and afterglow of europium-doped phosphors, such as  $\text{Dy}^{3+}$  and  $\text{Nd}^{3+}$  ions [13].

$\text{Sr}_4\text{Al}_2\text{O}_7$  with ratio of Al/Sr below 1 also has a potential to be hosts for rare earth metals. In this study, the  $\text{Sr}_4\text{Al}_2\text{O}_7:\text{Eu}^{2+}/\text{Dy}^{3+}$  phosphors were synthesized by a conventional solid-state reaction. The influences of concentration of  $\text{Dy}^{3+}$  ions and temperature on luminescent properties of  $\text{Sr}_4\text{Al}_2\text{O}_7:\text{Eu}^{2+}/\text{Dy}^{3+}$  phosphors were studied. As one of effective

✉ Zhijian Liu  
lzj6035@163.com

<sup>1</sup> Department of Power Engineering, School of Energy, Power and Mechanical Engineering, North China Electric Power University, Baoding 071003, People's Republic of China

<sup>2</sup> Department of Electrical Engineering, School of Electrical and Electronic Engineering, North China Electric Power University, Baoding 071003, People's Republic of China

synthesis methods for luminescence materials, solid state reaction can be operated simply, although the reaction temperature often is higher than other methods [14].

## 2 Experimental details

$\text{Sr}_4\text{Al}_2\text{O}_7:\text{Eu}^{2+}/\text{Dy}^{3+}$  phosphors were synthesized by the solid-state reaction. The dopant concentration of  $\text{Eu}^{2+}$  ion is 2 mol%. The mole ratios of  $\text{Dy}^{3+}$  and  $\text{Eu}^{2+}$  are 0, 1, 2, 3 and 4, respectively.  $\text{SrCO}_3$ ,  $\text{Al}_2\text{O}_3$ ,  $\text{Eu}_2\text{O}_3$  and  $\text{Dy}_2\text{O}_3$  were used as raw materials. Every starting material was of greater than 99.9 % purity. In the typical synthesis, starting materials were weighed according to the stoichiometric ratio and mixed in an aqueous medium for several hours using the ball–mill technique. After drying, the mixed powder was compacted into an alumina crucible. After closing the cover, the set of crucibles was loaded into a muffle furnace and calcined at the temperature of 1450 °C under a reducing environment (5 %  $\text{H}_2\text{-N}_2$ ). The system was kept at 1450 °C for 5 h and then cooled to room temperature naturally.

The characterizations of the synthesized phosphors were carried out using X-ray diffraction (XRD), scanning electron microscope (SEM), photo luminescent spectroscopy (PLS) and thermal luminescent spectroscopy (TLS). The XRD data were collected by a Bruker-AXS X-ray diffractometer (Cu  $K\alpha$ , 40 kV and 100 mA). The SEM image was obtained using a JSM 5410 microscope (JEOL, Japan). The luminescent properties were investigated by a LS50B photo luminescent spectrometer. A FJ427-A1 thermally stimulated spectrometer was used to reveal the afterglow behavior.

## 3 Results and discussion

Figure 1 gives the XRD pattern of  $\text{Sr}_4\text{Al}_2\text{O}_7:2 \text{ mol}\% \text{Eu}^{2+}/8 \text{ mol}\% \text{Dy}^{3+}$  phosphors. All diffraction peaks are well according with JCPDS Card No. 28-1204, indicating the successful synthesis of rare earth metals doped  $\text{Sr}_4\text{Al}_2\text{O}_7$  materials. Moreover, it can be seen from Fig. 1 that the doping rare earth metal ions do not influence the crystal phase-composition. All samples with different doped rare earth metal ions have similar XRD pattern. Figure 2 shows the SEM image of  $\text{Sr}_4\text{Al}_2\text{O}_7:2 \text{ mol}\% \text{Eu}^{2+}/8 \text{ mol}\% \text{Dy}^{3+}$  phosphors. The sample has the irregular morphology and wide size range, which is the common characterization for particles obtained by solid-state reaction. Also, the different doped rare earth metal ions have no obvious influence on morphology and size of samples.

Figure 3 gives the emission spectra of  $\text{Sr}_4\text{Al}_2\text{O}_7:2 - \text{mol}\% \text{Eu}^{2+}/x \text{ mol}\% \text{Dy}^{3+}$  ( $x = 0, 2, 4, 6$  and 8) phosphors

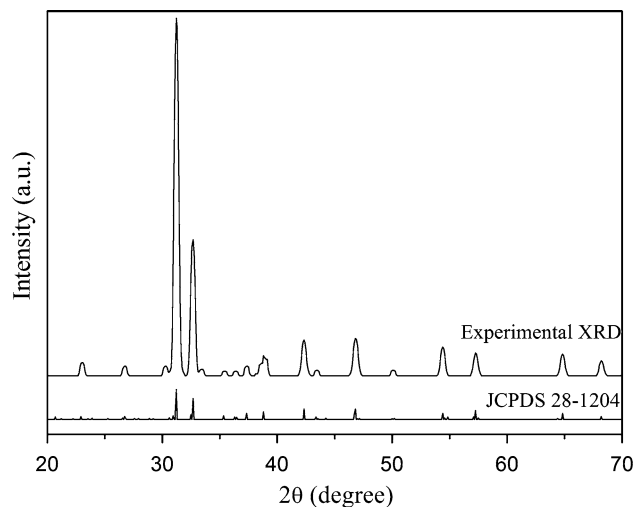


Fig. 1 XRD pattern of  $\text{Sr}_4\text{Al}_2\text{O}_7:2 \text{ mol}\% \text{Eu}^{2+}/8 \text{ mol}\% \text{Dy}^{3+}$  sample

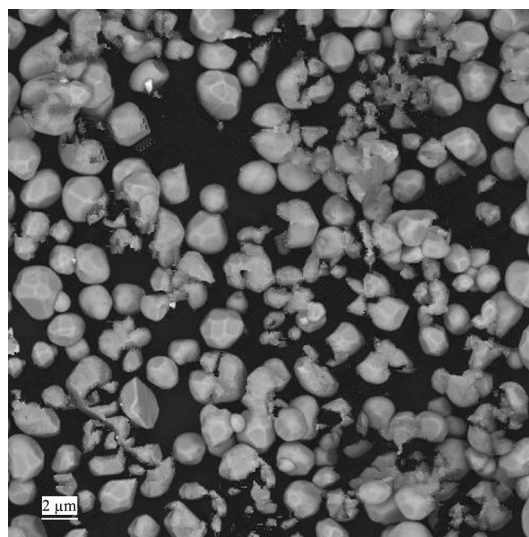
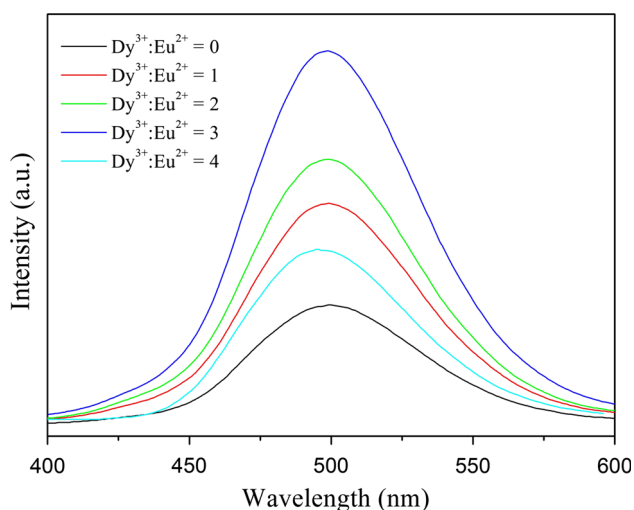


Fig. 2 SEM image of  $\text{Sr}_4\text{Al}_2\text{O}_7:2 \text{ mol}\% \text{Eu}^{2+}/8 \text{ mol}\% \text{Dy}^{3+}$  sample

under the excitation at 360 nm. All samples exhibit a broad emission band situated between 450 and 550 nm with a maximum at 499 nm, regardless of the  $\text{Dy}^{3+}/\text{Eu}^{2+}$  ratio. This emission originates from the  $4f^65d^1 \rightarrow 4f^7$  transition of electrons within  $\text{Eu}^{2+}$  ions. There is no emission bands can be ascribed to  $\text{Eu}^{3+}$  ions, indicating that  $\text{Eu}^{3+}$  ions are reduced to be  $\text{Eu}^{2+}$  ions completely. Herein, the  $\text{Eu}^{3+}$  ions in the crystal matrix are reduced easily to be  $\text{Eu}^{2+}$  ions, but  $\text{Dy}^{3+}$  ions are not reduced to be  $\text{Dy}^{2+}$  ions, which is caused by the different optical electro negativities for  $\text{Eu}^{3+}$  ions (1.74 eV) and  $\text{Dy}^{3+}$  ions (1.37 eV). The larger of the optical electro negativity leads to the lower the valence stability [8]. These induce that  $\text{Eu}^{3+}$  ions in the crystal matrix can be reduced easily to  $\text{Eu}^{2+}$  ions, but it is difficult for  $\text{Dy}^{3+}$  ions.



**Fig. 3** Emission spectra of  $\text{Sr}_4\text{Al}_2\text{O}_7:\text{Eu}^{2+}/\text{Dy}^{3+}$  samples with different mole ratios

Although the 4f electrons of  $\text{Eu}^{2+}$  ions are not sensitive to crystal lattice environment due to the shielding function of outer shell, the 5d electrons can easily coupled with crystal lattice, thus the 4f 5d hybridization state can be split by the influence of crystal field and coupled fiercely with crystal lattice phonon, which leads to a broad emission band. From Fig. 3, it can be seen that all samples containing  $\text{Dy}^{3+}$  ions have higher emission intensity than samples doped solely with  $\text{Eu}^{2+}$  ions. Moreover, the co-doped  $\text{Dy}^{3+}$  ions do not bring about the new emission bands, indicating that  $\text{Eu}^{2+}$  is the emission center in  $\text{Sr}_4\text{Al}_2\text{O}_7:\text{Eu}^{2+}/\text{Dy}^{3+}$  phosphors. The emission intensity increases with the increase of the mole ratio of  $\text{Dy}^{3+}/\text{Eu}^{2+}$  up to 3 and then decreases. The doped  $\text{Dy}^{3+}$  ions generate deeper trapping energy levels in the crystal matrix, which trap and store electrons. It disturbs the process of relaxation transitions of excited electrons of  $\text{Eu}^{2+}$  ions from excited state returning to ground state [15]. When the molar ratio of  $\text{Dy}^{3+}/\text{Eu}^{2+}$  reaches a certain value, the best synergistic effect between  $\text{Dy}^{3+}$  and  $\text{Eu}^{2+}$  ions is achieved. Meanwhile, both the density and depth of trapping and the amounts of stored electrons are appropriate and the best emission intensity is obtained corresponding to this value. However, for any higher  $\text{Dy}^{3+}/\text{Eu}^{2+}$  ( $>3$ ) ratios, the phenomenon of concentration quenching occurs, which results in decrease in emission intensity [16].

Figure 4 gives the thermoluminescence spectra of  $\text{Sr}_4\text{Al}_2\text{O}_7:2 \text{ mol}\% \text{Eu}^{2+}/x \text{ mol}\% \text{Dy}^{3+}$  ( $x = 0, 2, 4, 6$  and  $8$ ) phosphors. Thermoluminescence is an effective tool for some applications, such as dosimetry, age determination and geology defect structure analysis. Emission intensities for all samples increase firstly with the increases of temperature and then decrease. The peak positions and

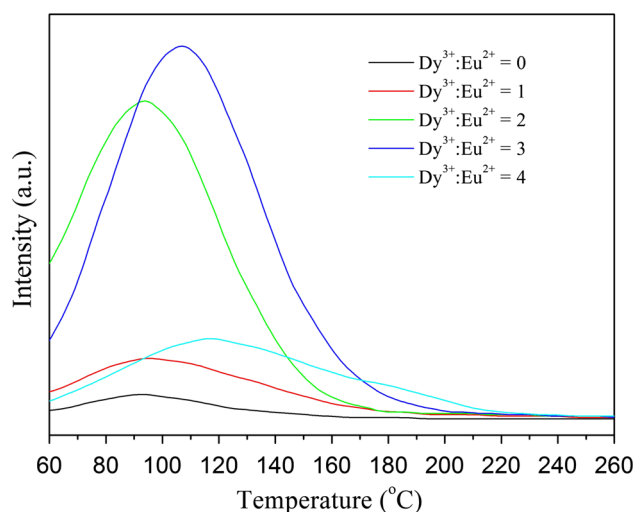


**Fig. 4** Thermoluminescence spectra of  $\text{Sr}_4\text{Al}_2\text{O}_7:\text{Eu}^{2+}/\text{Dy}^{3+}$  samples with different mole ratios

intensities of emissions are various with the different mole ratios of  $\text{Dy}^{3+}/\text{Eu}^{2+}$ .  $\text{Sr}_4\text{Al}_2\text{O}_7:2 \text{ mol}\% \text{Eu}^{2+}/6 \text{ mol}\% \text{Dy}^{3+}$  sample shows the highest emission intensity at about  $107^\circ\text{C}$ . Generally speaking, the depth and the density of electron traps, formed by the doped rare earth metal ions, have significant influence on the afterglow properties of phosphors in that long duration phosphorescence is dominated by the recombination process of the electrons, which were thermally released from the traps with the  $\text{Eu}^{2+}$  centers [17]. The trap depth and trap concentration in the phosphors can be obtained by analyzing the thermoluminescent spectra. Upon heating, the trapped electrons return to their normal lower-energy positions, releasing energy in the process. Emission intensity decreases when the mole ratio of  $\text{Dy}^{3+}/\text{Eu}^{2+}$  reaches a value of 4. The probable reason for such quenching may be the increase in probability of non-radiative transitions of the luminescent molecules from the excited state to the ground state in comparison to the probability of radiative transitions.

Figure 5 presents the decay curves of  $\text{Sr}_4\text{Al}_2\text{O}_7:2 \text{ mol}\% \text{Eu}^{2+}/x \text{ mol}\% \text{Dy}^{3+}$  ( $x = 0, 2, 4, 6$  and  $8$ ) phosphors. Theoretically, afterglow phenomenon is witnessed only when appropriate trap energy level exists. In case the trap energy level is shallow, electrons in the trap are excited easily and come back to the excited state, which results in short afterglow time. If the trap energy level is deeper, higher energy is needed when excited electrons in the trap come back to the excited state, so electrons are stored only in trap energy level and afterglow phenomenon is not observed. As shown in Fig. 5, all decay curves for  $\text{Sr}_4\text{Al}_2\text{O}_7:\text{Eu}^{2+}/\text{Dy}^{3+}$  phosphors include three different processes, namely fast, intermediate and subsequent slow-decaying process. The fast-decaying process is due to the shore

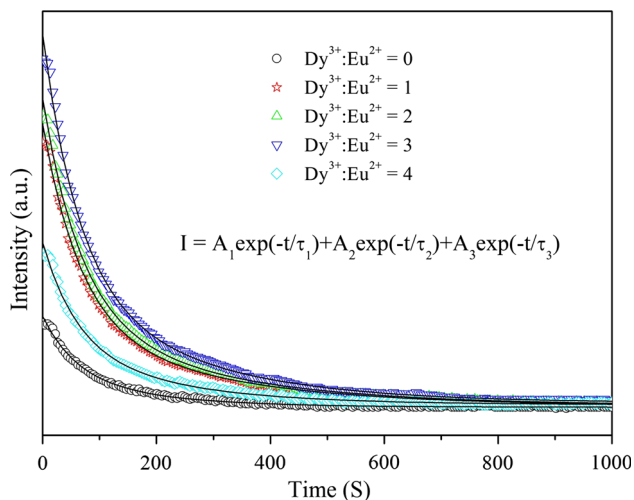


**Fig. 5** Decay curves of  $\text{Sr}_4\text{Al}_2\text{O}_7:\text{Eu}^{2+}/\text{Dy}^{3+}$  samples with different mole ratios

survival time of electrons in  $\text{Eu}^{2+}$  state while the slow-decaying process owes to the deep trap energy center of  $\text{Dy}^{3+}$  [18]. The  $\text{Eu}^{2+}$  and  $\text{Dy}^{3+}$  ions in aluminates phosphors are the luminescent centers and the traps respectively. The long afterglow property usually results from the trap energy level produced by doping of  $\text{Eu}^{2+}$  and  $\text{Dy}^{3+}$  ions in the crystals. It has been widely accepted that the  $\text{Dy}^{3+}$  in the  $\text{Eu}^{2+}$  co-doping system only serves as the trap center, not as the luminescent center in the hosts [19]. Many researchers have found that the co-doped  $\text{Dy}^{3+}$  can prolong the decay time greatly. Thus in the  $\text{Sr}_4\text{Al}_2\text{O}_7:\text{Eu}^{2+}/\text{Dy}^{3+}$  phosphors, the  $\text{Dy}^{3+}$  can also play the role of trap centers, which capture the free electrons to form metastable state and then release the trapped electrons upon thermal activation to recombine with the luminescent centers accompanying the luminescence. The decay curves corresponding to different phosphor samples indicate the initial luminescent intensity and afterglow decay rate to be different from each other, which are mainly influenced by the  $\text{Dy}^{3+}$  concentration and host structure. And the decay curves can fit well with the equation of  $I = A_1 \exp(-t/\tau_1) + A_2 \exp(-t/\tau_2) + A_3 \exp(-t/\tau_3)$ , where  $I$  is the intensity,  $A_1$ ,  $A_2$  and  $A_3$  are constants,  $t$  is time, and  $\tau_1$ ,  $\tau_2$  and  $\tau_3$  are decay times for fast, intermediate and slow exponential components, respectively [20]. The values of  $\tau_1$ ,  $\tau_2$  and  $\tau_3$  for  $\text{Sr}_4\text{Al}_2\text{O}_7:\text{Eu}^{2+}/\text{Dy}^{3+}$  samples are shown in Table 1.

#### 4 Conclusions

The long afterglow  $\text{Sr}_4\text{Al}_2\text{O}_7:\text{Eu}^{2+}/\text{Dy}^{3+}$  phosphors can be synthesized by solid-state reaction at 1450 °C. The phosphors synthesized at 1450 °C have pure  $\text{Sr}_4\text{Al}_2\text{O}_7$  phase. The SEM micrographs reveal that  $\text{Sr}_4\text{Al}_2\text{O}_7:\text{Eu}^{2+}/\text{Dy}^{3+}$  phosphors show similar irregular morphology. Under the

**Table 1** Decay times for  $\text{Sr}_4\text{Al}_2\text{O}_7:\text{Eu}^{2+}/\text{Dy}^{3+}$  samples

Sample	$\tau_1$ (s)	$\tau_2$ (s)	$\tau_3$ (s)
$\text{Sr}_4\text{Al}_2\text{O}_7:2 \text{ mol}\% \text{Eu}^{2+}$	53.02	139.85	518.62
$\text{Sr}_4\text{Al}_2\text{O}_7:2 \text{ mol}\% \text{Eu}^{2+}/2 \text{ mol}\% \text{Dy}^{3+}$	66.37	186.01	735.96
$\text{Sr}_4\text{Al}_2\text{O}_7:2 \text{ mol}\% \text{Eu}^{2+}/4 \text{ mol}\% \text{Dy}^{3+}$	108.52	240.29	826.38
$\text{Sr}_4\text{Al}_2\text{O}_7:2 \text{ mol}\% \text{Eu}^{2+}/6 \text{ mol}\% \text{Dy}^{3+}$	118.65	290.84	926.37
$\text{Sr}_4\text{Al}_2\text{O}_7:2 \text{ mol}\% \text{Eu}^{2+}/8 \text{ mol}\% \text{Dy}^{3+}$	58.23	162.35	638.51

excitation at 360 nm, all the  $\text{Sr}_4\text{Al}_2\text{O}_7:\text{Eu}^{2+}/\text{Dy}^{3+}$  phosphors exhibit a broad-band emission peaking at 499 nm. The emission intensity increases with the increasing mole ratio of  $\text{Dy}^{3+}/\text{Eu}^{2+}$  up to 3 and then decreases. The  $\text{Eu}^{2+}$  and  $\text{Dy}^{3+}$  ions in aluminates phosphors are the luminescent centers and the traps respectively. The presence of  $\text{Dy}^{3+}$  improves the afterglow considerably without modifying the wavelength of the emitted radiation. Thermoluminescence results and decay curves show that the traps generated by  $\text{Dy}^{3+}$  ions in these phosphors are deep.

**Acknowledgments** The work is supported by the Fundamental Research Funds for the Central Universities No. 2015MS108.

#### References

1. Y. Xu, Y. He, X. Yuan, Powder Technol. **172**, 99 (2007)
2. S.J. Kim, H.I. Won, N. Hayk, C.W. Won, D.K. Jeon, A.G. Kirakosyan, Mater. Sci. Eng. B. **176**, 1521 (2011)
3. P. Zhang, L. Li, Y. Tian, Phys. B **404**, 4286 (2009)
4. P. Huang, Q. Zhang, C. Cui, J. Li, Opt. Mater. **33**, 1252 (2011)
5. C. Chang, W. Li, X. Huang, Z. Wang, X. Chen, X. Qian, R. Guo, Y. Ding, D. Mao, J. Lumin. **130**, 347 (2010)
6. R.S. Garces, J.T. Torres, A.F. Valdes, Ceram. Int. **38**, 889 (2012)
7. E. Shafia, M. Bodaghi, S. Esposito, A. Aghaei, Ceram. Int. **40**, 4697 (2014)
8. A. Yu, D. Zhang, Y. Hu, J. Mater. Sci.: Mater. Electron. **25**, 4434 (2014)
9. K.E. Foka, F.B. Dejene, H.C. Swart, Phys. B **439**, 177 (2014)
10. W. Zhang, F. Liu, S. Feng, S. Hao, Y. Xu, J. Guan, J. Mater. Sci.: Mater. Electron. **25**, 2355 (2014)
11. S.Y. Kaya, E. Karacaoglu, B. Karasu, Ceram. Int. **38**, 3701 (2012)
12. F. Wei, Q. Jia, J. Mater. Sci.: Mater. Electron. **26**, 262 (2015)
13. T. Aitasalo, P. Deren, J. Holsa, H. Jungner, J.-C. Krupa, M. Lastusaari, J. Legendziewicz, J. Niittykoski, W. Strek, J. Solid State Chem. **171**, 114 (2003)
14. Y. Tang, X. Yang, Y. Xu, J. Mater. Sci.: Mater. Electron. **26**, 2311 (2015)
15. D.S. Kshatri, A. Khare, J. Alloys Compd. **588**, 488 (2014)
16. J. Zhang, M. Ge, J. Lumin. **131**, 1765 (2011)
17. Y.H. Lin, Z.T. Zhang, Z.L. Tang, J.Y. Zhang, Z.S. Zheng, X. Lu, Mater. Chem. Phys. **70**, 156 (2001)
18. Z. Qiu, Y. Zhou, M. Lü, A. Zhang, A. Zhang, Q. Ma, Acta Mater. **55**, 2615 (2007)
19. M. Fang, H. Wang, X. Tan, B. Cheng, L. Zhang, Z. Xiao, J. Alloys Compd. **457**, 413 (2008)
20. T. Katsumata, T. Nabae, K. Sasajima, S. Komuro, T. Morikawa, J. Electrochem. Soc. **144**, L243 (1997)